Amplitude and Phase Estimation of Backscatter Tag-to-Tag Channel

Abeer Ahmad†, Xiao Sha*, Akshay Athalye*, Samir Das†, Petar Djurić* and Milutin Stanaćević*

*Department of Electrical and Computer Engineering, Stony Brook University, Stony Brook, NY 11794
†Department of Computer Science, Stony Brook University, Stony Brook, NY 11794
Email: milutin.stanacevic@stonybrook.edu

Abstract—Large scale networks of intelligent sensors that can function without any batteries will have enormous implications in applications that range from smart spaces to structural and environmental monitoring. RF tags present an amenable platform for sensor integration as the backscatter communication offers low energy cost of communication. Current RF tags either use extremely low-power sensors or perform tasks of tag localization and identification based on the strength of the backscatter signal. We present a technique for estimation of amplitude and phase of the tag-to-tag channel that can be performed with very limited computational and energy resources. This enables monitoring of the interactions between tagged objects and activities around tags, as well as assessment of a variety of engineering structures. Experimental results demonstrate high resolution in the amplitude and phase channel measurement at a distances ranging from 22 cm to 1.34 m.

I. INTRODUCTION

Wireless channel estimation, in addition to enhancing the performance of a communication link, offers a sensing modality that is amenable to monitoring the surrounding environment [1], [2]. However, existing active or passive RF sensors have some important limitations in terms of spatial resolution, scalability and deployment. For granular and long-term monitoring, RF sensors have to be integrated in a small form factor and be self-powered. Conventional RFID tags provide near-zero power operation at a small-form factor but require deployment of costly RFID readers that limit the scalability of this approach [3]–[7]. Additionally, granularity of this approach is limited by the number of wireless reader-to-tag channels in this centralized system. RF sensors with active radio could provide granularity based on sensor-to-sensor channel estimation, but the power requirement for an active radio would prohibit the self-power operation of this type of sensors.

This leads to passive RF sensing integrated on RF tags that can talk to each other without the presence of a centralized device like a reader by way of backscattering an ambient RF signal [8]–[10]. If the power level of an ambient RF signal is not high enough for backscatter-based communication, a CW signal can be generated by a dedicated low-cost device, exciter, as illustrated in Figure 1. A RF tag with a transmitter based on a passive modulator and a receiver based on an envelope detector allows for extreme low-power cost for communication [11]–[13]. Passive RF sensing is enabled by the ability of the tags to estimate the RF parameters of the
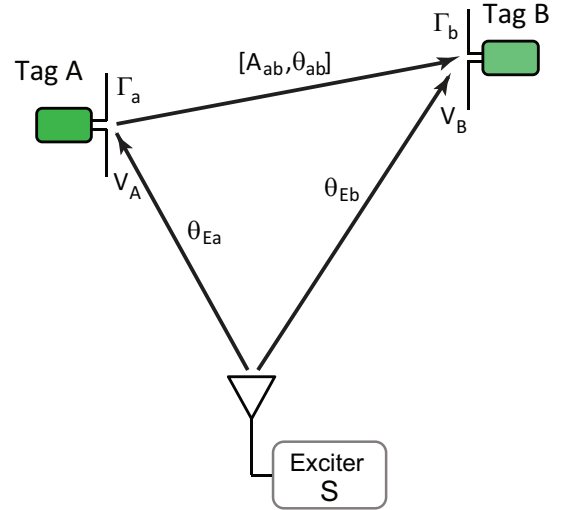

Fig. 1. Tag-to-tag channel.

wireless channel between pairs of communicating tags without the use of IQ demodulation.

A technique for the channel phase estimation in tag-to-tag link that estimates the joint phase of the exciter-tag channels and the tag-to-tag channel has been previously proposed [14], [15]. The technique has also been applied for the task of activity recognition [14]. In this paper, we present a technique that isolates the amplitude and phase of the tag-to-tag channel, leading to the invariance in the exciter position. This enables the use of the proposed technique in the task of monitoring the properties of the channel medium, that is the properties of the material in which RF tags are embedded.

II. TAG-TO-TAG CHANNEL ESTIMATION

The tag-to-tag link comprises a tag A and a tag B in a presence of CW signal, as illustrated in Figure 1. For simplicity, we assume that the source of CW signal is a dedicated RF exciter. The link is asymmetric, that is the properties of the link depend on the direction of the transmission. We first analyze the case in which we observe the receiving signal at the tag B and how it depends on the reflection of the tag A. The incident signal at the tag B comprises the direct path signal from the exciter and the signal reflected from the tag A. The tags integrate the envelope detector and extract the amplitude

of the received signal. Assuming that the amplitude of the signal from the exciter is much larger than the amplitude of the signal reflected from the tag A, the amplitude of the RF signal at the tag B, v_b, is

$$v_b = V_B + V_A A_{ab} |1 - \Gamma_a| \cos(\theta_{Ea} + \angle(1 - \Gamma_a) + \theta_{ab} - \theta_{Eb}) \quad (1)$$

where V_A and V_B are the amplitudes of the signal received from the exciter at the tags A and B, respectively, when the other tag is not present. Γ_a is the reflection coefficient of the tag A. A_{ab} and θ_{ab} are the amplitude and phase of the tag-to-tag channel. Assuming only direct path, A_{ab} can be according to Friis RF signal propagation equation expressed as

$$A_{ab} = \sqrt{G_a G_b} \frac{\lambda}{4\pi d}, \quad (2)$$

where G_a and G_b are the antenna gains of tags A and B, respectively. The antenna gain is the function of the orientation of the antenna. The channel phase, θ_{ab}, is

$$\theta_{ab} = 2\pi \frac{d}{\lambda}, \quad (3)$$

where λ is the wavelength of the CW signal. θ_{Ea} and θ_{Eb} represent the phase of the exciter-tag A and exciter-tag B channel, respectively. In this model, we neglect the reflections from the environment. However, due to the CW excitation signal, the form of the equations stays the same with the inclusion of the reflections from the environments. The amplitude and the phase of the exciter-tag A, exciter-tag B and tag-to-tag channel change due to the reflections. Including the magnitude and phase of the reflection coefficient Γ_a, (1) becomes

$$\begin{aligned} v_b = V_B \quad &+ \quad V_A A_{ab} \cos(\theta_{Ea} + \theta_{ab} - \theta_{Eb}) \quad (4) \\ &- \quad V_A A_{ab} |\Gamma_a| \cos(\theta_{Ea} + \theta_{ab} - \theta_{Eb} + \phi_a) \end{aligned}$$

where ϕ_a is the phase of the reflection coefficient Γ_a.

To estimate the unknown channel amplitude and phase, we vary the phase of the reflection coefficient at tag A, ϕ_a, and measure the amplitude of the received signal, v_b, at tag B. This measurement requires a modified modulator and demodulator design of RF tag [14]. While the traditional backscatter modulator transmits data by switching between two different impedances connected to the antenna, for passively measuring channel parameters the modulator will switch between a range of impedances. The modulator will be implemented as a multi-port switch with terminating impedances that enable the total reflection at different phase angles. For each reflection phase $\phi_{a,k}$, the amplitude of the incident RF signal at Rx tag, $v_{b,k}$ is recorded. This calls for analog-to-digital converter(ADC) of the baseband signal at a demodulator after the envelope detection. The energy cost of ADC conversion at the demodulator is low, as ADCs with 8-bit resolution at kSamples/s sampling rate consume 10s nW of power [15]–[17].

From N measurements with different reflection coefficients $\Gamma_{a,k}$ we obtain N equations:

$$\begin{bmatrix} v_{b,1} \\ v_{b,2} \\ .. \\ v_{b,N} \end{bmatrix} = H_1 \begin{bmatrix} V_B \\ V_A A_{ab} \cos(\Theta_1) \\ V_A A_{ab} \sin(\Theta_1) \end{bmatrix} \quad (5)$$
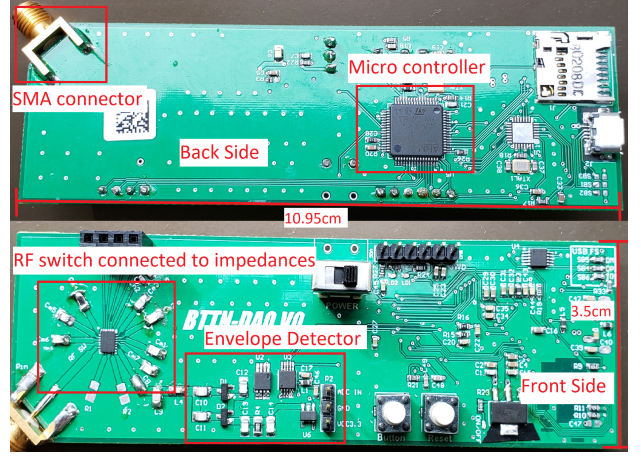

Fig. 2. Discrete implementation of RF tag used in experiments.

where $\Theta_1 = \theta_{Ea} + \theta_{ab} - \theta_{Eb}$ and

$$H_1 = \begin{bmatrix} 1 & 1 - |\Gamma_{a,1}| \cos(\phi_{a,1}) & |\Gamma_{a,1}| \sin(\phi_{a,1}) \\ 1 & 1 - |\Gamma_{a,2}| \cos(\phi_{a,2}) & |\Gamma_{a,2}| \sin(\phi_{a,2}) \\ .. & & \\ 1 & 1 - |\Gamma_{a,N}| \cos(\phi_{a,N}) & |\Gamma_{a,N}| \sin(\phi_{a,N}) \end{bmatrix}. \quad (6)$$

From (5), we obtain estimates $\hat{V}_B$, $\hat{\Theta}_1$ and $(V_A \hat{A}_{ab})$ as

$$\begin{bmatrix} \hat{V}_B \\ (V_A \hat{A}_{ab}) \cos(\hat{\Theta}_1) \\ (V_A \hat{A}_{ab}) \sin(\hat{\Theta}_1) \end{bmatrix} = W_1 \begin{bmatrix} V_{b,1} \\ V_{b,2} \\ .. \\ V_{b,N} \end{bmatrix}, \quad (7)$$

where $W_1 = (H_1^T H_1)^{-1} H_1^T$.

These estimated values don't provide estimates of the amplitude and phase of the tag-to-tag channel. However, if we observe the received signal at tag A as a function of the reflection coefficient at tag B, $\Gamma_{b,k}$, we obtain estimates $\hat{V}_A$, $\hat{\Theta}_2$ and $(V_B \hat{A}_{ab})$, where $\Theta_2 = \theta_b + \theta_{ab} - \theta_a$. When the tag B reflection coefficient is set to $\Gamma_{b,k}$, the received signal amplitude at tag A, $v_{a,k}$ is written in a similar manner to (5)

$$v_{a,k} = V_A + V_B A_{ab} \cos(\Theta_2) - V_B A_{ab} |\Gamma_{b,k}| \cos(\Theta_2 + \phi_{b,n}), \quad (8)$$

From N measurements, we obtain estimates $\hat{V}_A$, $\hat{\Theta}_2$ and $(V_B \hat{A}_{ab})$ as

$$\begin{bmatrix} \hat{V}_A \\ (V_B \hat{A}_{ab}) \cos(\hat{\Theta}_2) \\ (V_B \hat{A}_{ab}) \sin(\hat{\Theta}_2) \end{bmatrix} = W_2 \begin{bmatrix} V_{a,1} \\ V_{a,2} \\ .. \\ V_{a,N} \end{bmatrix}, \quad (9)$$

where $W_2 = (H_2^T H_2)^{-1} H_2^T$ and

$$H_2 = \begin{bmatrix} 1 & 1 - |\Gamma_{b,1}| \cos(\phi_{b,1}) & |\Gamma_{b,1}| \sin(\phi_{b,1}) \\ 1 & 1 - |\Gamma_{b,2}| \cos(\phi_{b,2}) & |\Gamma_{b,2}| \sin(\phi_{b,2}) \\ .. & & \\ 1 & 1 - |\Gamma_{b,N}| \cos(\phi_{b,N}) & |\Gamma_{b,N}| \sin(\phi_{b,N}) \end{bmatrix}. \quad (10)$$
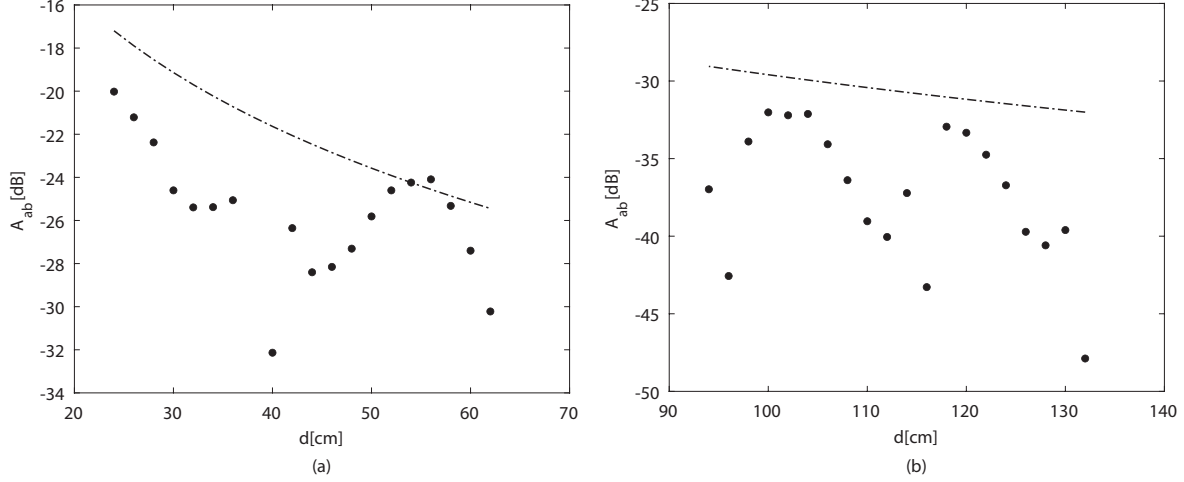
Fig. 3. Estimated channel amplitude as a function of distance between tags. The dashed line shows the channel attenuation according to the Friis RF signal propagation model.
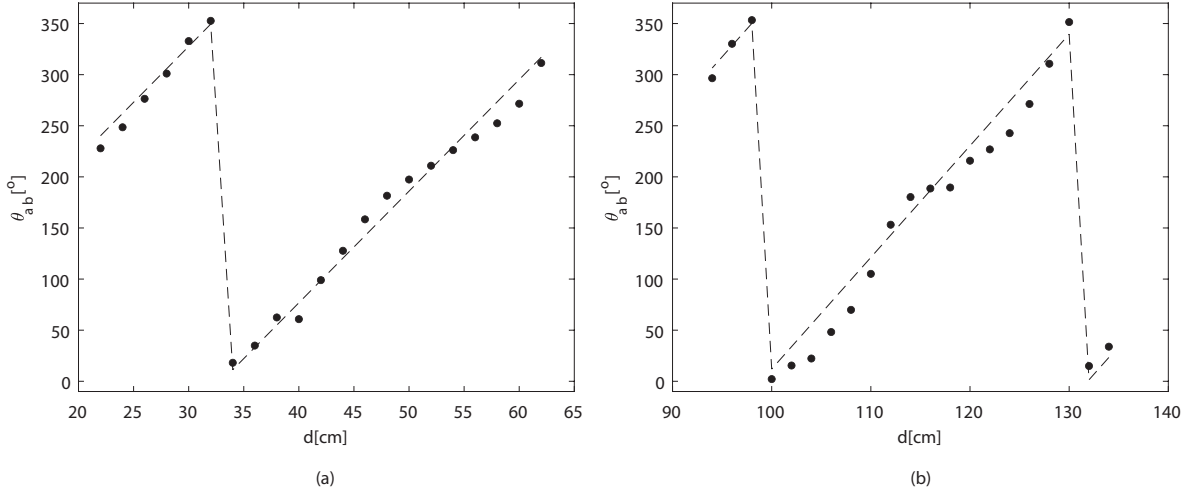

Fig. 4. Estimated channel phase as a function of distance between tags. The dashed line shows the true channel phase at each distance.

From the obtained estimates, the channel parameters A_{ab} and θ_{ab} are obtained as

$$\hat{\theta}_{ab} = \left(\frac{\hat{\Theta}_1 + \hat{\Theta}_2}{2} \right) \mod \pi, \qquad (11)$$

$$\hat{A}_{ab} = \frac{1}{2} \left(\frac{(V_B \hat{A}_{ab})}{\hat{V}_B} + \frac{(V_A \hat{A}_{ab})}{\hat{V}_A} \right), \qquad (12)$$

where $\hat{\theta}_{ab}$ is wrapped phase in the range from 0 to π.

III. LIMITS IN PASSIVE CHANNEL ESTIMATION

The resolution of the passive estimation of amplitude and phase of tag-to-tag channel is limited by the resolution of the reflection amplitude and phase on the side of the backscattering tag, the resolution of the ADC in discriminating the incident baseband signal at the receiving tag, as well as

the channel noise and the interference. To maximize the received signal, each terminating impedance in the modulator of backscattering tag should lead to the reflection coefficient with magnitude close to the unity. The reflection phases, $\phi_{a,k}$, span the range from -π to π. The number of different terminating impedances is a trade-off between the estimation resolution, power consumption and time required for the phase estimation. We have previously demonstrated that 8 different phases are sufficient for phase estimation in applications like activity recognition [14]. However, in a static environment in applications like structural monitoring, the amplitude and phase have to be estimated with a finer resolution, calling for a larger number of terminating impedance. The increase in the number of terminating impedances is possible using RF tag implementation in the application specific integrated circuits(ASIC). In addition to the resolution, the required time
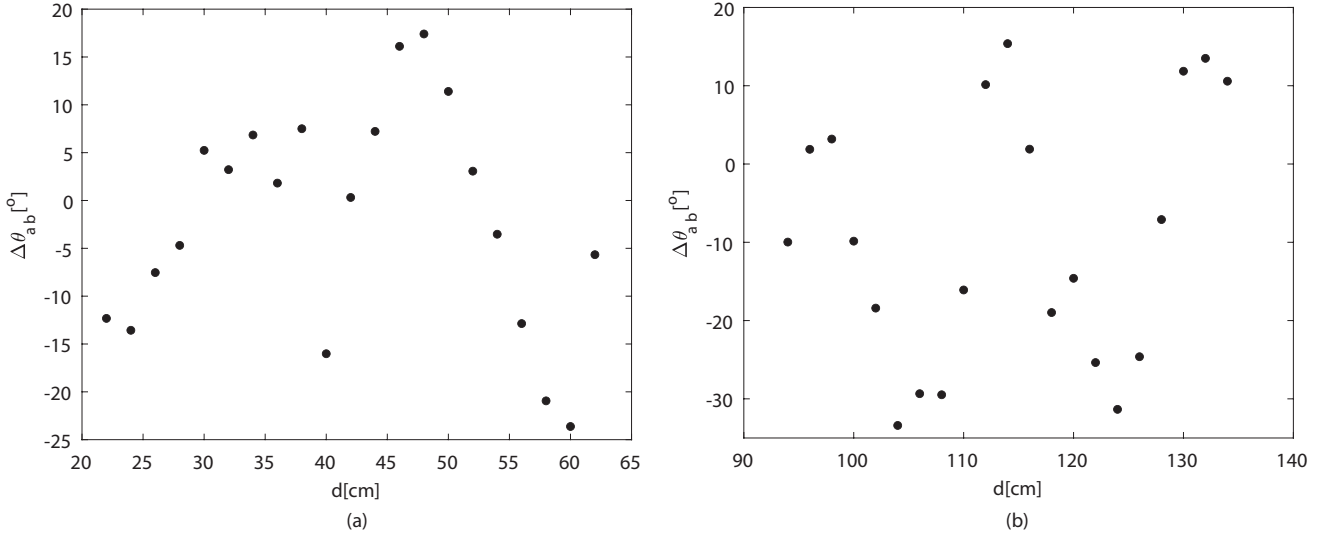
Fig. 5. Estimated channel phase error as the function of distance between the tags.

IV. EXPERIMENTAL RESULTS

To evaluate the performance of the proposed passive technique for estimating the tag-to-tag channel amplitude and phase, we have performed a set of experiments. In all the experiments, we have used a discrete implementation of the RF tag, shown in Figure 2 which interfaces a dipole antenna. The RF tag implements a multiphase modulator and demodulator based on the envelope detector. The multi-phase modulator integrates a multi-port RF switch terminated, in addition to open-circuit and 50 Ω, with seven impedances, preselected to provide the phases of the reflection coefficient evenly spaced in a range of 2π. The demodulator implementation includes the envelope detector followed by a low-pass filter and a 16-bit 1 MSample/s analog-to-digital (ADC) converter. The digitized amplitude of the input RF signal is then transferred to a PC for data analysis.

We perform experiments in an indoor environment where the size of the room is 5m x 3m x 2.5m. One tag is kept at a fixed location, while the second tag moves along a rail. The input power of the sliding tag is in the range from -15 dBm to -18 dBm, while the exciter operated at CW frequency of 915 MHz. For each inter-tag distance, we collect digitized baseband signal at both tags for each of 8 reflecting phases of the opposing tag. The amplitude and phase of the tag-to-tag channel are then estimated off-line on PC based on the recorded voltage values. The experiments are performed for the distance between tags in the range from 22 cm to 62 cm with 2 cm step, as well as in the range from 94 cm to 134 cm with the same step. The obtained estimated channel attenuation is shown in Figure 3. We can observe that the estimated

attenuation follows the Friis RF signal propagation model, as well as the effect of the reflection in the environement on the channel attenuation. The estimated phase of the tag-to-tag channel for two ranges in the inter-tag distance is shown in Figure 4. The dashed line shows the true wrapped channel phase at each distance. The ambiguity of the phase wrapping has to be resolved in applications like tag localization. Figure 5 shows the phase error as a function of the distance between tags.

For a single distance between tags, we repeat the measurement 20 times and the measured standard deviation, that stems from the channel noise and electronic noise, is 1.9^o. The measured standard deviation of the phase error, shown in Figure 5, is 14.5^o, leading to the conclusion that the error in the distance measurement is dominated by the reflections in the tag-to-tag channel.

V. CONCLUSIONS

We envision that the intelligent RF tags will be distributed through an environment and that they will coherently sense the environment, process the sensed data, and communicate with each other. Further, they will learn from the environment, make inference, make decisions, and act on them, overall making the space around them "smart." These capabilities put together will radically change the way we interact with the physical world. Additionally, the monitoring of infrastructure such as buildings, roads and bridges becomes continuous and seamless making it more resource-efficient and environmentally friendlier and safer.

REFERENCES

[1] H. Meyr, M. Moeneclaey, and S. Fechtel, *Digital communication receivers: synchronization, channel estimation, and signal processing.* John Wiley & Sons, Inc., 1997.

[2] Y. Li, N. Seshadri, and S. Ariyavisitakul, "Channel estimation for ofdm systems with transmitter diversity in mobile wireless channels," *IEEE Journal on Selected areas in communications*, vol. 17, no. 3, pp. 461–471, 1999.

[3] S. Kim, C. Mariotti, F. Alimenti, P. Mezzanotte, A. Georgiadis, A. Collado, L. Roselli, and M. M. Tentzeris, "No battery required: Perpetual rfid-enabled wireless sensors for cognitive intelligence applications," *IEEE Microwave magazine*, vol. 14, no. 5, pp. 66–77, 2013.

[4] A. P. Sample, D. J. Yeager, P. S. Powledge, A. V. Mamishev, and J. R. Smith, "Design of an rfid-based battery-free programmable sensing platform," *IEEE transactions on instrumentation and measurement*, vol. 57, no. 11, pp. 2608–2615, 2008.

[5] D. Yeager, A. Sample, and J. Smith, "Wisp: A passively powered uhf rfid tag with sensing and computation," *RFID Handbook: Applications, Technology, Security, and Privacy*, pp. 261–278, 2008.

[6] H. Zhang, J. Gummeson, B. Ransford, and K. Fu, "Moo: A batteryless computational rfid and sensing platform," *University of Massachusetts Computer Science Technical Report UM-CS-2011-020*, 2011.

[7] M. Buettner, B. Greenstein, and D. Wetherall, "Dewdrop: an energy-aware runtime for computational rfid," in *Proc. USENIX NSDI*, 2011, pp. 197–210.

[8] V. Liu, A. Parks, V. Talla, S. Gollakota, D. Wetherall, and J. R. Smith, "Ambient backscatter: Wireless communication out of thin air," *ACM SIGCOMM Computer Communication Review*, vol. 43, no. 4, pp. 39–50, 2013.

[9] A. N. Parks, A. Liu, S. Gollakota, and J. R. Smith, "Turbocharging ambient backscatter communication," *ACM SIGCOMM Computer Communication Review*, vol. 44, no. 4, pp. 619–630, 2014.

[10] J. Ryoo, J. Jian, A. Athalye, S. R. Das, and M. Stanaćević, "Design and evaluation of "bttn": a backscattering tag-to-tag network," *IEEE Internet of Things Journal*, vol. 5, no. 4, pp. 2844–2855, 2018.

[11] C. Boyer and S. Roy, "Backscatter communication and rfid: Coding, energy, and mimo analysis," *IEEE Transactions on Communications*, vol. 62, no. 3, pp. 770–785, 2014.

[12] J. Griffin and G. Durgin, "Complete link budgets for backscatter-radio and rfid systems," *IEEE Trans. on Antennas and Propagation Magazine*, vol. 51, no. 2, pp. 11–25, 2009.

[13] Y. Karimi, A. Athalye, S. Das, P. Djurić, and M. Stanaćević, "Design of backscatter-based tag-to-tag system," in *IEEE International Conference on RFID (RFID)*, 2017.

[14] J. Ryoo, Y. Karimi, A. Athalye, M. Stanaćević, S. Das, and P. Djurić, "Barnet: Towards activity recognition using passive backscattering tag-to-tag network," in *Proceedings of the 16th Annual International Conference on Mobile Systems, Applications, and Services.* ACM, 2018, pp. 414–427.

[15] Y. Karimi, Y. Huang, A. Athalye, S. Das, P. Djurić, and M. Stanaćević, "Passive wireless channel estimation in rf tag network," in *2019 IEEE International Symposium on Circuits and Systems (ISCAS)*. IEEE, 2019, pp. 1–5.

[16] H.-C. Hong and G.-M. Lee, "A 65-fj/conversion-step 0.9-v 200-ks/s rail-to-rail 8-bit successive approximation adc," *IEEE Journal of Solid-State Circuits*, vol. 42, no. 10, pp. 2161–2168, 2007.

[17] J. Sauerbrey, D. Schmitt-Landsiedel, and R. Thewes, "A 0.5-v 1-uw successive approximation adc," *IEEE Journal of Solid-State Circuits*, vol. 38, no. 7, pp. 1261–1265, 2003.